Check for
updates

Spectral Engineering for Optimal Signal Performance in the Microwave SQUID Multiplexer

J. M. Salum[1,2,3] · **M. E. García Redondo**[1,2,3,5] · **L. P. Ferreyro**[1,2,3,5] ·
J. Bonilla-Neira[1,3,4] · **N. Müller**[1,3,4] · **J. M. Geria**[1,3,4,5] · **J. Bonaparte**[2,6] ·
T. Muscheid[2] · **R. Gartmann**[2] · **A. Fuster**[1,5,6] · **A. Almela**[1,5,6] · **M. R. Hampel**[1,5,6] ·
L. E. Ardila-Perez[2] · **O. Sander**[2] · **S. Kempf**[2,4] · **M. Platino**[1,3,6] · **M. Weber**[2,4] ·
A. Etchegoyen[1]

Abstract

We describe a technique to optimize the dynamic performance of microwave SQUID multiplexer (μMUX)-based systems. These systems proved to be adequate for reading out multiple cryogenic detectors simultaneously. However, the requirement for denser detector arrays to increase the sensitivity of scientific experiments makes its design a challenge. When modifying the readout power, there is a trade-off between decreasing the signal-to-noise ratio (SNR) and boosting the nonlinearities of the active devices. The latter is characterized by the spurious free dynamic range (SFDR) parameter and manifests as an increment in the intermodulation products and harmonics power. We estimate the optimal spectral location of the SQUID signal containing the detector information for different channels. Through the technique, what we refer to as *Spectral Engineering*, it is possible to minimize the SNR degradation while maximizing the SFDR of the detector signal, thus, overcoming the trade-off.

Keywords Cryogenic detectors · Microwave SQUID multiplexing · Signal processing · Spectral engineering

1 Introduction

The high sensitivity of cryogenic detectors makes them ideal for a wide range of scientific applications including particle physics, astrophysics, and materials science. Based on the scientific topic of interest, the detectors are designed to measure energy (calorimeters) like the magnetic microcalorimeters (MMC) [1] or power (bolometers) like the recently proposed magnetic microbolometers (MMB) [2]. Cosmic microwave background (CMB) surveys like QUBIC (Q & U Bolometric

---

Extended author information available on the last page of the article

Interferometer for Cosmology) [3] utilize bolometers to measure the B mode polarization of the CMB. Experiments which seek to detect the energy of an emitted particle use calorimeters. For example, ECHo (Electron Capture in ^{163}Ho) [4] aims to establish a new upper limit of the neutrino mass in the sub-eV range through the electron capture process of ^{163}Ho. A dedicated multiplexer based on superconducting quantum interference devices (SQUID) is typically designed to readout arrays of cryogenic detectors. This system is called microwave SQUID multiplexer (μMUX), [5] and it is designed to multiplex as many detectors as possible in different frequency channels within a given bandwidth using a frequency division multiplexing (FDM) technique. Each channel is composed of a unique superconducting resonator coupled through a radio frequency (RF) SQUID to cryogenic detectors. Room temperature electronics (RTE) designed in a software defined radio (SDR) scheme synthesize and condition a frequency comb to monitor all the μMUX channels.

To meet the demand for increasingly sensitive detection systems, more densely populated detector arrays are required. This makes the readout system design more complex since multiple factors must be optimized. For example, one of the challenges to overcome is the trade-off between the signal-to-noise ratio (SNR) and spurious free dynamic range (SFDR) [6]. Keeping the same readout power per channel, the total tone comb power increases with the amount of channels, which raise the power of intermodulation products and harmonics in the active devices. Similarly, the SFDR, specifying the amplitude relation between the signal of interest and the worst spurious signal in the spectrum, is reduced. In contrast, if the readout power per channel decreases, a degradation of the SNR occurs in the RTE as well as in the μMUX if the readout power is below the optimal value [7]. This could diminish the sensitivity of the detection system, therefore contradicting the reason for increasing the density of the detector array.

In this article, we present a technique called *spectral engineering* to overcome this trade-off. It consists of locating the SQUID signal containing the detector information in the spectral band that optimizes SNR and SFDR of the detector signal.

2 Concept

As described in Sect. 1, a multi-tonal signal is synthesized to monitor all channels in the μMUX. Each tone drives a different channel formed by a unique resonator filter coupled to a SQUID which is at the same time coupled to a cryogenic detector. A sawtooth-shaped magnetic flux signal (FR) is synthesized to drive all the SQUIDs and linearize their responses [8]. Hence, the signal generated by each detector is translated to a phase shift of the SQUID response. Therefore, the μMUX imprints the detector's information to the multi-tonal signal in a process that involves two levels of modulation. The first modulation is given by the periodic variation of the magnitude and phase of each channel given by the FR. The second modulation occurs in the SQUID and as a consequence of mixing both the FR and the magnetic flux generated by the detector. The frequency comb is then reconditioned and processed in the RTE to recover first the SQUID signal and then the detector signal for each channel. In Fig. 1, a sketch of the processed SQUID signal spectrum is given.
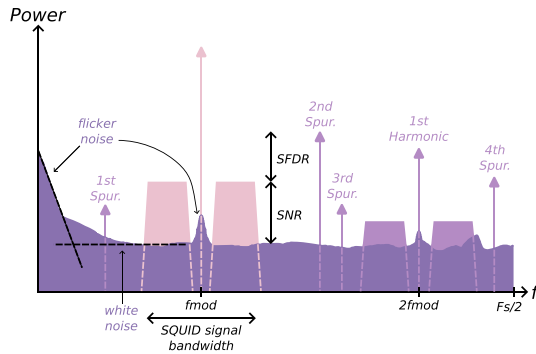
Fig. 1 An illustration of a typical SQUID signal spectral profile after downconverting it with the monitor tone. The SQUID signal is shown in pink and is formed by a carrier signal and its phase modulation, the detector signal. The carrier frequency is defined by the FR as $f_{mod} = N_{\Phi_0} f_{ramp}$. In dark violet, the white noise and flicker noise contributions are shown. In light violet, undesired signals are shown in the spectrum due to spurious, intermodulation products, harmonics, etc.

The SQUID signal carrier frequency (f_{mod}) is defined by the FR frequency (f_{ramp}) and amplitude in terms of number of magnetic flux quanta (N_{Φ_0}) as $f_{mod} = N_{\Phi_0} f_{ramp}$ [9]. Since the ultimate goal is to recover the detector signal, the SNR and SFDR parameters are considered relative to it (see Fig. 1). Noise components such as white noise and flicker noise determine the SNR. Undesired components like spurious signals and the SQUID signal harmonics define the SFDR value. Different SNR and SFDR values can be obtained experimentally for the particular set of hardware by adjusting the f_{mod} value. It is desired that both SNR and SFDR parameters are positive and large.

Despite each channel in the µMUX having a different spectrum profile, a value for f_{ramp} and N_{Φ_0} can be found to maximize the SNR and SFDR for the worst case and at the same time set a lower limit for the rest of the channels.

3 Measurements

3.1 Experimental Setup

In Fig. 2a, we show the used RTE. It consists of the commercial evaluation board ZCU102 build around a Multi-Processor System-on-Chip (MPSoC) and the converter board AD-FMCDAQ2 that generate and process the tone comb. A custom microwave board [10] up-converts the tone comb to the µMUX frequency band. The µMUX is shown in Fig. 2b. It has nine channels between 4 and 8 GHz separated every 500 MHz. In Fig. 2c, the transmission parameter (S_{21}) of the µMUX is plotted.

Since the current electronics allows an instantaneous readout bandwidth of 800 MHz, we measured three different channels one after the other at around 3.965 GHz (ch0), 5.954 GHz (ch4) and 6.456 GHz (ch5). A channelizer based on a Goertzel filter [13] was implemented for separating each monitor tone. In order
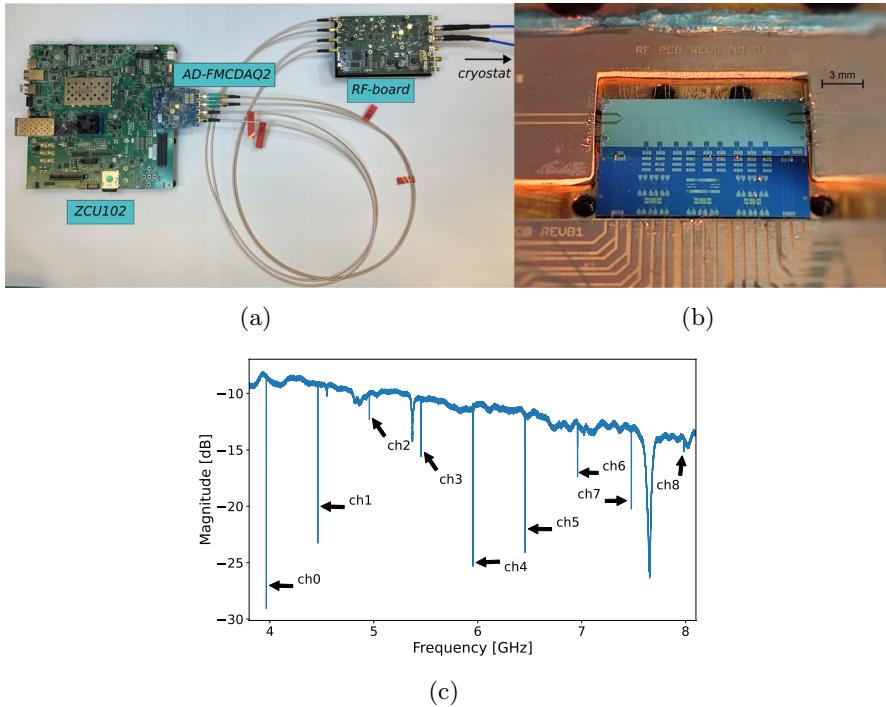
(a)　　　　　　　　　　　　　　(b)

(c)

Fig. 2 **a** RTE, composed of two commercial boards (ZCU102 [11], AD-FMCDAQ2 [12]) and a custom RF-board [10]. **b** The µMUX used for the measurements. It has nine channels distributed between 4 and 8 GHz. For scientific purposes, channels 2, 3, 4, 7 and 8 have different input coils attached to the SQUIDs, meanwhile channels 0, 1, 5 and 6 do not have it. **c** The µMUX S_{21} parameter. Apart from the channel resonances, also a resonance between channels 2 and 3 and between channels 7 and 8 is present that correspond to the cavity resonance of the sample holder

not to lose generality in this technique, no magnetic flux signal was concatenated into the SQUID, and we assumed the noise power and spurious signals do not change when magnetic flux signal is present. Therefore, we acquired noise and nonlinearity contributions of the RTE and the µMUX (see Fig. 3).

Fig. 3 Power spectral density of the monitor signal related to ch5 after the channelizer. The power is referenced to the monitor tone power, thus, expressed in dBc units. The pink shaded area indicates the region in frequency across which the center frequency of the boxcar filter was varied
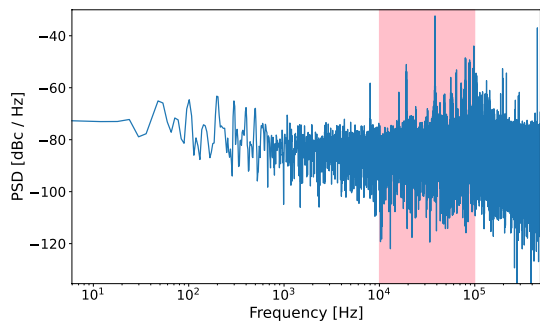
To find the optimal f_{mod} that maximizes the SNR and SFDR values of the detector signal, we emulated different conditions for the SQUID signal carrier frequency and bandwidth. We calculated the total spectrum power of the signal in Fig. 3 after filtering it with a rectangular window for the different conditions. The rectangular window filter was chosen since it is the standard [7, 8, 14–16] to recover the detector signal from the µMUX. Although, it is not the best window filter to attenuate the harmonics of the SQUID signal as explained in [9]. The center frequency of the boxcar filter (which should match the f_{mod} frequency) was varied between 10 and 100 kHz in steps of 5.96 Hz. Afterward, we obtained the optimal f_{mod} value which results in the lowest sum of noise power and spurious power. Another parameter that was also varied is the boxcar filter bandwidth. This parameter should match the SQUID signal bandwidth which depends on the amplitude and bandwidth of the detector signal. As mentioned in Sect. 1, there are many projects that use this readout technique for cryogenic detectors. These projects cover different detector bandwidths that can range from Hz to MHz regimes. For this work, we chose boxcar filter bandwidths between 10 and 5000 Hz.

3.2 Results

The results obtained are displayed in Fig. 4. It shows the integrated spectrum power for the different boxcar filter bandwidths and central frequencies. In addition, for each calculated power, only the worst case was plotted among the three measured channels, i.e., the highest power. Each spectrum power trace per detector bandwidth was normalized to the minimum power of each one (dBc$_{min}$) so the best situation occurs when the calculated spectrum power is 0 dBc' (where dBc' = dBc − dBc$_{min}$). These cases, which indicate the optimal f_{mod} value, were marked with circles in Fig. 4. Considering the overall spectral power, an enhancement of up to 50 dB can be obtained if the optimal f_{mod} value is set against the worst case. If only the noise
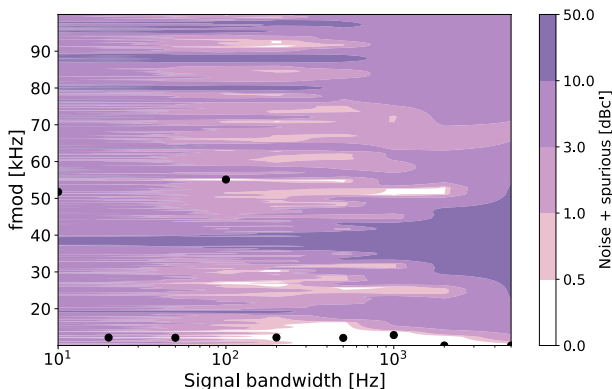

Fig. 4 Spectrum power for the different boxcar filter central frequencies (or f_{mod}) and bandwidths (or SQUID signal bandwidth). In color, the total spectrum power (noise + spurious) for the worst case among the three measured channels is showed. Therefore, the f_{mod} value that maximizes the SNR and SFDR is marked with circles

contributions are considered, setting the optimal f_{mod} value improves up to 7 dB against the worst case.

4 Conclusions

In this work, we present a technique to overcome the trade-off between the signal-to-noise ratio (SNR) and the spurious free dynamic range (SFDR) in the microwave SQUID multiplexer (μMUX)-based systems. This technique seeks to optimize both parameters by placing the SQUID signal in the spectral region that maximize the detector SNR and SFDR or what we call *Spectral Engineering*. By this technique, we demonstrated an improvement of up to 50 dB and 7 dB comparing the optimal case against the worst one considering the total spectrum power and only the noise contributions, respectively.

Declarations

Conflict of interest The authors declare no competing interests.

References

1. A. Fleischmann, C. Enss, G.M. Seidel, Metallic magnetic calorimeters, in *Topics in Applied Physics* (Springer, Berlin, 2005), pp. 151–216. https://doi.org/10.1007/10933596_4
2. J.M. Geria, M.R. Hampel, S. Kempf, J.J.F. Bonaparte, L.P. Ferreyro, M.E.G. Redondo, D.A. Almela, J.M.S. Salum, N.A. Müller, J.D.B. Neira, A.E. Fuster, M. Platino, A. Etchegoyen, Suitability of magnetic microbolometers based on paramagnetic temperature sensors for CMB polarization measurements. J. Astron. Telesc. Instrum. Syst. (2023). https://doi.org/10.1117/1.jatis.9.1.016002
3. ...L. Mousset, M.M.G. Lerena, E.S. Battistelli, P. Bernardis, P. Chanial, G. D'Alessandro, G. Dashyan, M.D. Petris, L. Grandsire, J.-C. Hamilton, F. Incardona, S. Landau, S. Marnieros, S. Masi, A. Mennella, C. O'Sullivan, M. Piat, G. Ricciardi, C.G. Scóccola, M. Stolpovskiy, A. Tartari, J.-P. Thermeau, S.A. Torchinsky, F. Voisin, M. Zannoni, P. Ade, J.G. Alberro, A. Almela, G. Amico, L.H. Arnaldi, D. Auguste, J. Aumont, S. Azzoni, S. Banfi, A. Baù, B. Bélier, D. Bennett, L. Bergé,

J.-P. Bernard, M. Bersanelli, M.-A. Bigot-Sazy, J. Bonaparte, J. Bonis, E. Bunn, D. Burke, D. Buzi, F. Cavaliere, C. Chapron, R. Charlassier, A.C.C. Cerutti, F. Columbro, A. Coppolecchia, G.D. Gasperis, M.D. Leo, S. Dheilly, C. Duca, L. Dumoulin, A. Etchegoyen, A. Fasciszewski, L.P. Ferreyro, D. Fracchia, C. Franceschet, K.M. Ganga, B. García, M.E.G. Redondo, M. Gaspard, D. Gayer, M. Gervasi, M. Giard, V. Gilles, Y. Giraud-Heraud, M.G. Berisso, M. González, M. Gradziel, M.R. Hampel, D. Harari, S. Henrot-Versillé, E. Jules, J. Kaplan, C. Kristukat, L. Lamagna, S. Loucatos, T. Louis, B. Maffei, S. Mandelli, W. Marty, A. Mattei, A. May, M. McCulloch, L. Mele, D. Melo, L. Montier, L.M. Mundo, J.A. Murphy, J.D. Murphy, F. Nati, E. Olivieri, C. Oriol, A. Paiella, F. Pajot, A. Passerini, H. Pastoriza, A. Pelosi, C. Perbost, M. Perciballi, F. Pezzotta, F. Piacentini, L. Piccirillo, G. Pisano, M. Platino, G. Polenta, D. Prêle, R. Puddu, D. Rambaud, E. Rasztocky, P. Ringegni, G.E. Romero, J.M. Salum, A. Schillaci, S. Scully, S. Spinelli, G. Stankowiak, A.D. Supanitsky, P. Timbie, M. Tomasi, C. Tucker, G. Tucker, D. Viganò, N. Vittorio, F. Wicek, M. Wright, A. Zullo, QUBIC II: spectral polarimetry with bolometric interferometry. J. Cosmol. Astropart. Phys. **2022**(04), 035 (2022). https://doi.org/10.1088/1475-7516/2022/04/035

4. L. Gastaldo et al., The electron capture in 163Ho experiment: ECHo. Eur. Phys. J. Spec. Top. **226**(8), 1623–1694 (2017). https://doi.org/10.1140/epjst/e2017-70071-y

5. J.A.B. Mates, The microwave SQUID multiplexer. Ph.D. thesis, University of Colorado Boulder, 2011. https://scholar.colorado.edu/concern/graduate_thesis_or_dissertations/gt54kn14d

6. ...C. Yu, Z. Ahmed, J.C. Frisch, S.W. Henderson, M. Silva-Feaver, K. Arnold, D. Brown, J. Connors, A.J. Cukierman, J.M. D'Ewart, B.J. Dober, J.E. Dusatko, G. Haller, R. Herbst, G.C. Hilton, J. Hubmayr, K.D. Irwin, C.-L. Kuo, J.A.B. Mates, L. Ruckman, J. Ullom, L. Vale, D.D.V. Winkle, J. Vasquez, E. Young, Slac microresonator rf (smurf) electronics: a tone-tracking readout system for superconducting microwave resonator arrays. Rev. Sci. Instrum. **94**, 014712 (2022). https://doi.org/10.1063/5.0125084

7. C. Schuster, M. Wegner, S. Kempf, Simulation framework for microwave SQUID multiplexer optimization. J. Appl. Phys. **133**(4), 044503 (2023). https://doi.org/10.1063/5.0135124

8. J.A.B. Mates, K.D. Irwin, L.R. Vale, G.C. Hilton, J. Gao, K.W. Lehnert, Flux-ramp modulation for SQUID multiplexing. J. Low Temp. Phys. **167**(5–6), 707–712 (2012). https://doi.org/10.1007/s10909-012-0518-6

9. J.M. Salum, T. Muscheid, A. Fuster, M.E.G. Redondo, M.R. Hampel, L.P. Ferreyro, J.M. Geria, J. Bonilla-Neira, N. Müller, J. Bonaparte, A. Almela, L.E. Ardila-Perez, M. Platino, O. Sander, M. Weber, Aliasing effect on flux ramp demodulation: nonlinearity in the microwave squid multiplexer. J. Low Temp. Phys. **213**(3–4), 223–236 (2023). https://doi.org/10.1007/s10909-023-02993-z

10. R. Gartmann, N. Karcher, R. Gebauer, O. Krömer, O. Sander, Progress of the ECHo SDR readout hardware for multiplexed MMCs. J. Low Temp. Phys. (2022). https://doi.org/10.1007/s10909-022-02854-1

11. D.H. Xilinx, *ZCU102 Evaluation Board User Guide* (Advanced Micro Devices, Inc., 2023). Advanced Micro Devices, Inc.. Ver. 1.7. https://www.xilinx.com/support/documents/boards_and_kits/zcu102/ug1182-zcu102-eval-bd.pdf

12. D. Analog, AD-FMCDAQ2-EBZ User Guide. Analog Devices (2023). Analog Devices. Ver. 4. https://wiki.analog.com/resources/eval/user-guides/ad-fmcdaq2-ebz

13. L.P. Ferreyro, M.G. Redondo, M.R. Hampel, A. Almela, A. Fuster, J. Salum, J.M. Geria, J. Bonaparte, J. Bonilla-Neira, N. Müller, N. Karcher, O. Sander, M. Platino, M. Weber, A. Etchegoyen, An implementation of a channelizer based on a goertzel filter bank for the read-out of cryogenic sensors. J. Instrum. **18**(06), 06009 (2023). https://doi.org/10.1088/1748-0221/18/06/p06009

14. D.P. Richter, Multikanal-Auslesung von metallischen magnetischen Kalorimetern mittels eines vollständigen Mikrowellen-SQUID-Multiplexer-Systems. Ph.D. thesis, Kirchhoff Institute for Physics, July 2021. https://doi.org/10.11588/heidok.00030266

15. D.T. Becker, D.A. Bennett, M. Biasotti, M. Borghesi, V. Ceriale, M.D. Gerone, M. Faverzani, E. Ferri, J.W. Fowler, G. Gallucci, J.D. Gard, A. Giachero, J.P. Hays-Wehle, G.C. Hilton, J.A.B. Mates, A. Nucciotti, A. Orlando, G. Pessina, A. Puiu, C.D. Reintsema, D.R. Schmidt, D.S. Swetz, J.N. Ullom, L.R. Vale, Working principle and demonstrator of microwave-multiplexing for the HOLMES experiment microcalorimeters. J. Instrum. **14**(10), 10035–10035 (2019). https://doi.org/10.1088/1748-0221/14/10/p10035

16. J.D. Gard, D.T. Becker, D.A. Bennett, J.W. Fowler, G.C. Hilton, J.A.B. Mates, C.D. Reintsema, D.R. Schmidt, D.S. Swetz, J.N. Ullom, A scalable readout for microwave SQUID multiplexing of transition-edge sensors. J. Low Temp. Phys. **193**(3–4), 485–497 (2018). https://doi.org/10.1007/s10909-018-2012-2

Publisher's Note Springer Nature remains neutral with regard to jurisdictional claims in published maps and institutional affiliations.

Authors and Affiliations

J. M. Salum[1,2,3] · **M. E. García Redondo**[1,2,3,5] · **L. P. Ferreyro**[1,2,3,5] ·
J. Bonilla-Neira[1,3,4] · **N. Müller**[1,3,4] · **J. M. Geria**[1,3,4,5] · **J. Bonaparte**[2,6] ·
T. Muscheid[2] · **R. Gartmann**[2] · **A. Fuster**[1,5,6] · **A. Almela**[1,5,6] · **M. R. Hampel**[1,5,6] ·
L. E. Ardila-Perez[2] · **O. Sander**[2] · **S. Kempf**[2,4] · **M. Platino**[1,3,6] · **M. Weber**[2,4] ·
A. Etchegoyen[1]

✉ J. M. Salum
  juan.salum@iteda.cnea.gov.ar

1   Instituto de Tecnologías en Detección y Astropartículas (ITeDA), Buenos Aires, Argentina

2   Institute for Data Processing and Electronics (IPE), Karlsruhe Institute of Technology (KIT),
     Karlsruhe, Germany

3   Universidad Nacional de San Martín (UNSAM), Buenos Aires, Argentina

4   Institute of Micro- and Nanoelectronic Systems (IMS), Karlsruhe Institute of Technology (KIT),
     Karlsruhe, Germany

5   Universidad Tecnológica Nacional (UTN), Facultad Regional Buenos Aires, Buenos Aires,
     Argentina

6   Comisión Nacional de Energía Atómica (CNEA), Buenos Aires, Argentina